ELSEVIER

Journal of Power Sources 68 (1997) 145–152

JOURNAL OF POWER SOURCES

Synthesis and electrochemical properties of lithium iron oxides with layer-related structures

Ryoji Kanno *, Takayuki Shirane, Yukishige Inaba, Yoji Kawamoto

Department of Chemistry, Faculty of Science, Kobe University, Nada, Kobe, Hyogo 657, Japan

Accepted 13 November 1996

Abstract

Two modifications of layered lithium iron oxides were synthesized and characterized by X-ray diffractometry and electrochemical measurements. $LiFeO_2$ with α-$NaFeO_2$ structure was synthesized by the ion-exchange reaction in molten salts; cationic distribution in the host, α-$NaFeO_2$, affects the disordering in the reaction product. However, lithium de-intercalation was not confirmed. The ion-exchange reaction in molten salts gave a whole range of solid solution, $Li(Fe_{1-x}Ni_x)O_2$, using the α-$Na(Fe_{1-x}Ni_x)O_2$ hosts, and their electrochemical properties were determined. Lithium iron oxide, $LiFeO_2$, with a corrugated layer structure, was synthesized by an ion-exchange reaction between γ-FeOOH and $LiOH \cdot H_2O$. Lithium cells consisting of $LiFeO_2$ cathodes and lithium anodes showed good charge and discharge reversibility in the voltage 1.5–3.0 V range. © 1997 Published by Elsevier Science S.A.

Keywords: Lithium batteries; Insertion electrodes; Iron oxides; Layered structure

1. Introduction

Transition metal oxides $LiMO_2$ ($M = 3d$ transition metal) with the layered rocksalt structure have been studied for possible use as insertion electrodes in 4 V rechargeable lithium batteries. In this structure, alternate layers of Li and M occupy the octahedral sites of a cubic close packed (c.c.p.) oxygen array, making a rhombohedral structure.

Among these oxides, the iron system has advantages over layered-rocksalt cathodes such as $LiNiO_2$ and $LiCoO_2$ because they are non-toxic and cheaper. Iron oxide spinels have been studied as the possible candidates [1–5]. However, close packed spinel host and the tetrahedrally coordinated iron ions restrict the mobility of lithium at ambient temperature. To date, several materials have been proposed based on iron systems: layered oxyhalide FeOCl [6], derivatives prepared from FeOCl having γ-FeOOH structure [7], NASICON-type $Fe_2(SO_4)_3$ [8], and $LiFePO_4$ with the ordered olivine-type structure [8,9]. Our approach of new materials search for the iron system is focused on those having similar structures to the layered $LiCoO_2$ and $LiMnO_2$.

Fig. 1 shows the structure field map for AMO_2 compounds. The structures of $LiMO_2$ compounds are primarily dependent on the size of the M cation; $LiMO_2$ with M = V, Cr, Co, and Ni has a layered rocksalt structure [10–14], while the compounds containing Fe and Ti adopt a disordered cubic rocksalt structure or a tetragonally ordered structure [15–17]. The boundary of these two structure-types is located between V^{3+} (ionic radius $r = 0.640$) and Fe^{3+} ($r = 0.645$, high spin state). This means that if we chose a synthesis technique which enables us to make meta-stable phase compound, it

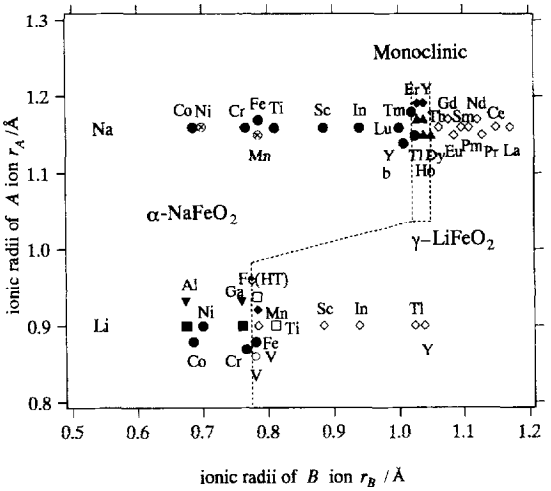

Fig. 1. Structure field map for AMO_2 compounds: (●) α-$NaFeO_2$ (rhombohedral); (▼) high-pressure phase; (⊗) α-$NaFeO_2$ (monoclinic); (○) high-pressure phase; (■) Wurtzite ($LiGaO_2$), β-GeO_2 ($LiAlO_2$); (□) NaCl (disorder); (▲) monoclinic; (◇) $LiFeO_2$ (tetragonal); (◆) orthorhombic (corrugated layer), and HT: high-temperature phase.

* Corresponding author.

PII S0378-7753(96)02625-0

might be possible to obtain either layered or a corrugated layer lithium iron oxides.

The compound $LiFeO_2$ synthesized by ion-exchange reactions in molten salts [18–20] has recently been clarified as a layered rocksalt-type by neutron diffraction and magnetic measurements [21]. However, the electrochemical characterization indicated no lithium de-intercalation from the host lattice.

Compounds with the composition $LiMO_2$ can have another layered structure; $LiMnO_2$ has a corrugated layer structure consisting of a c.c.p. oxygen array and cation sheets made up of alternating pairs of Li and Mn rows [22]. Recently, $LiMnO_2$ synthesized from an ion-exchange reaction between γ-MnOOH and $LiOH \cdot H_2O$ showed good electrochemical performance in lithium secondary cells [23,24]. Iron oxyhydroxides (FeOOH) have similar structures to those of the manganese system [25]; the α-, β-, and γ-type modifications have a small tunnel (α-MnOOH type), a large tunnel (α-MnO_2 type), and a corrugated layer (γ-MnOOH type) structure, respectively. We recently obtained $LiFeO_2$ with the corrugated structure which is electrochemically active [26].

We report here the synthesis of two modifications of $LiFeO_2$ with a corrugated layer structure and the α-$NaFeO_2$ structure, using an ion-exchange reaction. Relationship between the ion-exchange conditions and product structures is discussed based on the X-ray diffraction (XRD) results. Furthermore, the solid solution $Li(Fe_{1-x}Ni_x)O_2$ with the α-$NaFeO_2$ structure was synthesized and their electrochemical properties were clarified.

2. Experimental

2.1. Synthesis

2.1.1. $LiFeO_2$ and $Li(Ni_{1-x}Fe_x)O_2$ with a layered structure

The ternary oxide, α-$NaFeO_2$, was prepared by heating appropriate molar ratios of Na_2O_2 and γ-Fe_2O_3 (Na_2O_2, Wako Pure Chemical Industry, >95.3% purity; γ-Fe_2O_3, Toda Kogyo Company). These were mixed, pelletized in an argon-filled glove-box, and then heated at 300 to 600 °C in an oxygen atmosphere.

The solid solution, $NaFe_{1-x}Ni_xO_2$, was synthesized by heating appropriate molar ratios of Na_2O_2, γ-Fe_2O_3, and NiO (NiO, Nakarai Company, >99.9% purity). They were mixed, pelletized and heated at 800 °C in oxygen atmosphere for 30 h. Ion-exchange reactions were performed using molten salts, LiCl/KCl, LiCl/KCl/$BaCl_2$, $LiNO_3$, and $LiNO_3$/KNO_3. These were put into an alumina crucible and heated to the reaction temperature; the α-$NaFeO_2$ powders were then put into the molten salts. After the reaction, the crucible was quenched to room temperature and the salts were washed with hot water. The energy dispersion X-ray (EDX) analysis of $LiFeO_2$ revealed no Na left in the sample, indicating a complete ion-exchange reaction.

2.1.2. $LifeO_2$ with the corrugated layer structure

Starting materials used were $LiOH \cdot H_2O$, LiOH, and γ-FeOOH ($LiOH \cdot H_2O$, LiOH, Wako Pure Chemical Industry, >99.9% purity; γ-FeOOH, Toda Kogyo Company).

Ion-exchange reactions were performed using various molar ratios of the starting materials. These were mixed in appropriate molar ratios, put into a silver or gold tube and heated to a reaction temperature of 100–500 °C. After the reaction, the tube was quenched to room temperature. Unreacted lithium hydroxides were washed with cold water and the product dried in a desiccator.

2.2. Characterization

XRD patterns of powdered samples were obtained with an X-ray diffractometer (Rigaku RAD-C, 12 kW) using Cu Kα radiation. Lattice parameters were refined by Rietveld analysis using the computer program RIETAN [27]. The diffraction data were collected for 5 s at each 0.05° step width over a 2θ range from 10° to 100°. After electrochemical testing, samples were mounted on a specially designed X-ray holder in an argon atmosphere. A 7 μm thick aluminum window covered the sample holder in an arc to prevent moisture attack during measurements. The electrochemical intercalation and de-intercalation reactions were carried out using lithium cells. The working electrode consisted of a mixture of 50 mg sample, 10 mg acetylene black and 0.1 mg Teflon powder pressed into a tablet of 13 mm diameter under a pressure of 9 MPa. The cells used for electrochemical tests were constructed in a stainless-steel 2016 coin-type configuration. The separator employed was a microporous polypropylene sheet. Typical electrolytes used in these cells were 1 M solutions of $LiClO_4$ in a 50:50 mixture of propylene carbonate (PC) and 1,2-dimethoxyethane (DME) (Mitsubishi Petrochemical Company, battery grade) by volume. Electrochemical measurements were carried out at room temperature after standing overnight under zero current flow. Cell properties were measured galvanostatically.

3. Results and discussion

3.1. $LiFeO_2$ with α-$NaFeO_2$ structure

Previously, we indicated that layered $LiFeO_2$ obtained from α-$NaFeO_2$ synthesized at 550 °C and an ion-exchange reaction at 380 °C in LiCl/KCl showed a two-phasic property with α-$NaFeO_2$ type and a spinel-related type structures [21]. The two-phasic property is also confirmed with the results of Mössbauer and SQUID measurements, while the anti-ferromagnetic behavior was quite similar to that of α-$NaFeO_2$, which indicates the layered nature of the compound. However, de-intercalation from $LiFeO_2$ was not observed. In order to obtain monophasic properties, cationic disordering in the host, α-$NaFeO_2$, was reduced using lower synthesis temperatures of 350–500 °C.

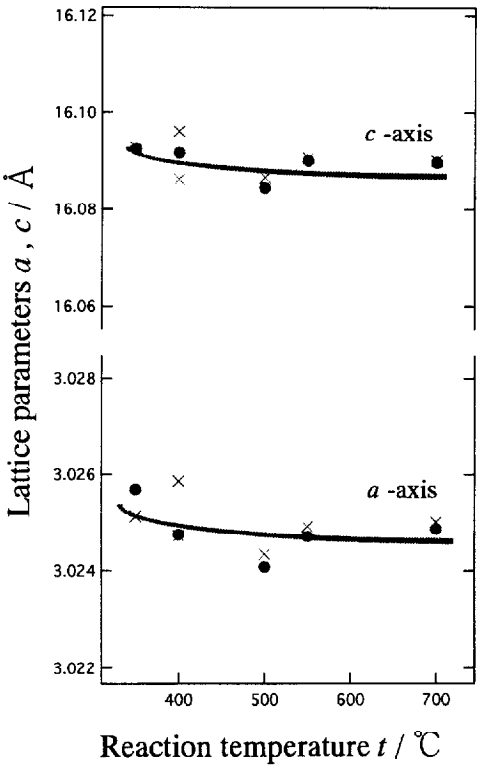

Fig. 2. Lattice parameters for α-$NaFeO_2$ synthesized at various temperatures.

Fig. 2 shows the synthesis temperature dependence of the lattice parameters for α-$NaFeO_2$ obtained at temperatures from 350 to 800 °C. The lattice parameters increased slightly with decreasing synthesis temperatures, suggesting the decrease in the amount of disordered Fe^{3+} ions (ionic radius $r = 0.645$ Å) in the Na sites (ionic radius (Na^+) $r = 1.02$ Å). X-ray Rietveld refinement results on these systems, however, gave no information about the disordering, because the difference in the scattering factors between Na and Fe ions is not large enough to distinguish the cationic distribution.

Ion-exchange reactions were carried out under various conditions. Fig. 3 shows the XRD pattern of the products under various reaction periods, temperatures, and molten salts. The sample with high crystallinity, having no impurity phase, was obtained for the reaction at 360–400 °C for 10 min to 1 h in LiCl/KCl molten salts.

Fig. 4(a) shows the lattice parameters of $LiFeO_2$ versus reaction temperature of the host materials. The lattice parameters decrease with decreasing synthesis temperatures of α-$NaFeO_2$, suggesting that the cation disorder in $LiFeO_2$ is dependent on those of the host material. Fig. 4(b) shows the lattice parameters as a function of disorder, x, in $Li_{1-x}Fe_{1+x}O_2$ determined by the Rietveld analysis. The structures were refined using a model that situates the disordered Fe ion only in the Li site. The parameters decrease with decreasing x, and the best sample obtained in the present study still contained about 5% of disorder.

Charge/discharge experiments of the Li/$LiFeO_2$ cells showed a very small charge/discharge capacity of $y = 0.1$ in $Li_{1-y}FeO_2$. However, a slightly different capacity and a

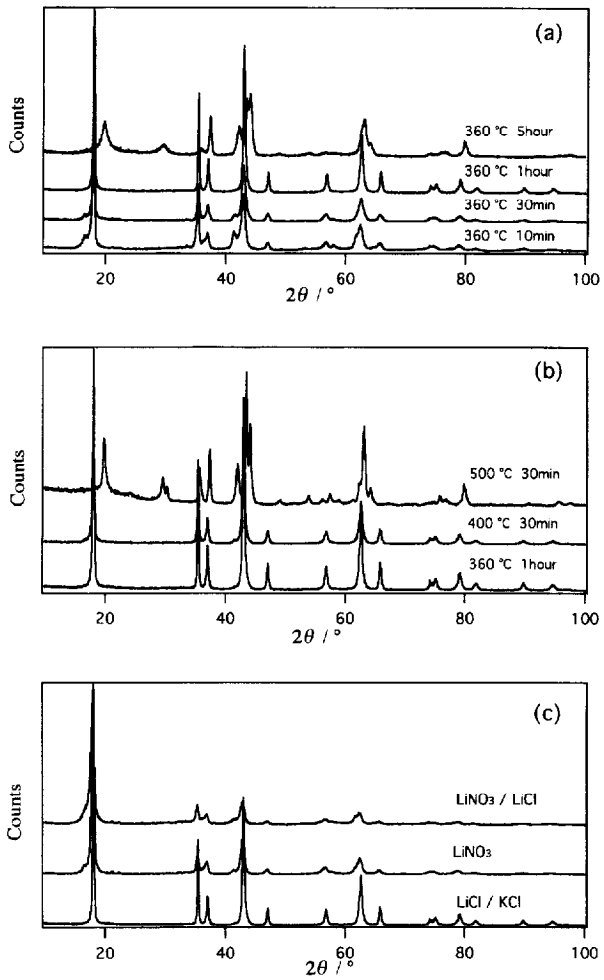

Fig. 3. XRD patterns for $LiFeO_2$ synthesized at various ion-exchange conditions: (a), (b) ion exchange in LiCl/KCl molten salt, and (c) ion-exchange with reaction conditions at 360 °C and 1 h.

shape of the charge/discharge curves between the samples $Li_{0.95}Fe_{1.05}O_2$ and $Li_{0.92}Fe_{1.08}O_2$ indicates that the cation disorder affects the charge/discharge characteristics. However, lithium de-intercalation was not confirmed by the XRD method in the present study. Further effort to reduce the disordering is neceassary.

3.2. $LiFeO_2 - LiNiO_2$ solid solution

The lithium nickel oxide $LiNiO_2$ has an ideal layered structure when the samples were carefully prepared [14,23], while layered $LiFeO_2$ still contained disorder in the Li sites. The solid solution between $LiNiO_2$ and $LiFeO_2$ might give us information on the $LiFeO_2$ structure if we clarify the structural changes through the solid solution. Furthermore, electrochemical characteristics of the solid solutions are also of interest. Reimers et al. [28] reported that the solid solution $Li_xFe_yNi_{1-y}O_2$ synthesized directly from the starting materials, $LiNO_3$, $Fe(NO_3)_2 \cdot 6H_2O$, and $Ni(CO_3)_2 \cdot 6H_2O$ had the layered rocksalt structure only in the composition range $0 \le x \le 0.23$; for $0.23 \le y \le 0.48$ phase coexistence occurs between hexagonal $LiFe_{0.23}Ni_{0.77}O_2$ and a cubic phase with

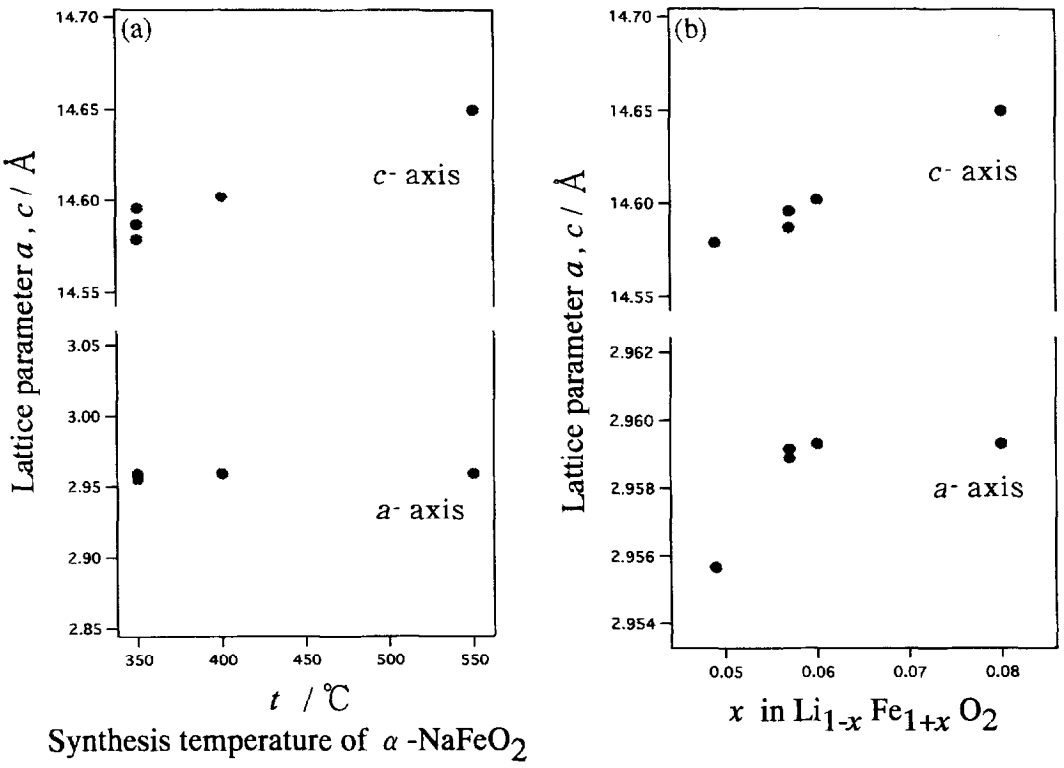

Fig. 4. Lattice parameters of $LiFeO_2$ as a function of (a) reaction temperature of the host material, and (b) as a function of cationic disordering, x, in $Li_{1-x}Fe_{1+x}O_2$.

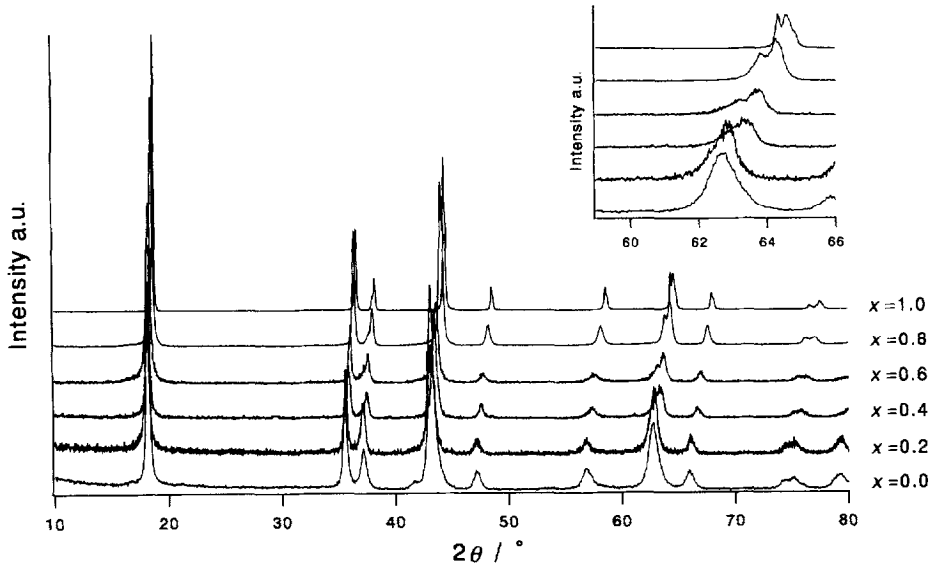

Fig. 5. XRD patterns for $LiFe_{1-x}Ni_xO_2$.

disordered rocksalt structure. Since the ion-exchange reaction of $NaFeO_2$ in molten salts led to the 'layered rocksalt' structure, formation of the whole range of solid solution might be expected. In the present study, we synthesized $LiFe_{1-x}Ni_xO_2$ from $NaFe_{1-x}Ni_xO_2$.

The solid solution $LiFe_{1-x}Ni_xO_2$ was synthesized at 400 °C using ion exchange in LiCl/KCl molten salts. The reaction products show monophasic properties for the whole range of the solid solution with the layered rocksalt structure. Fig. 5 shows the XRD peaks near $2\theta = 64°$. The peaks in the Ni-rich region of $1.0 \geq x \geq 0.4$ are separated into two peaks which are indexed as 110_{hexa} and 107_{hexa} reflections. However, the separation decreases from $x = 0.4$ to $x = 0.0$, and the peak at $x = 0.0$ could be indexed by both the hexagonal (110_{hexa} and 107_{hexa}) and the cubic (440_{cub}) cells. The lattice parameters increase with decreasing x from 1.0 to 0.0 for samples synthesized by ion exchange (see Fig. 6). However, no change was observed for samples synthesized by the solid-state reaction for $x \geq 0.8$. This indicates that the ion-exchange reaction gave a layered structure in the whole range of the solid solu-

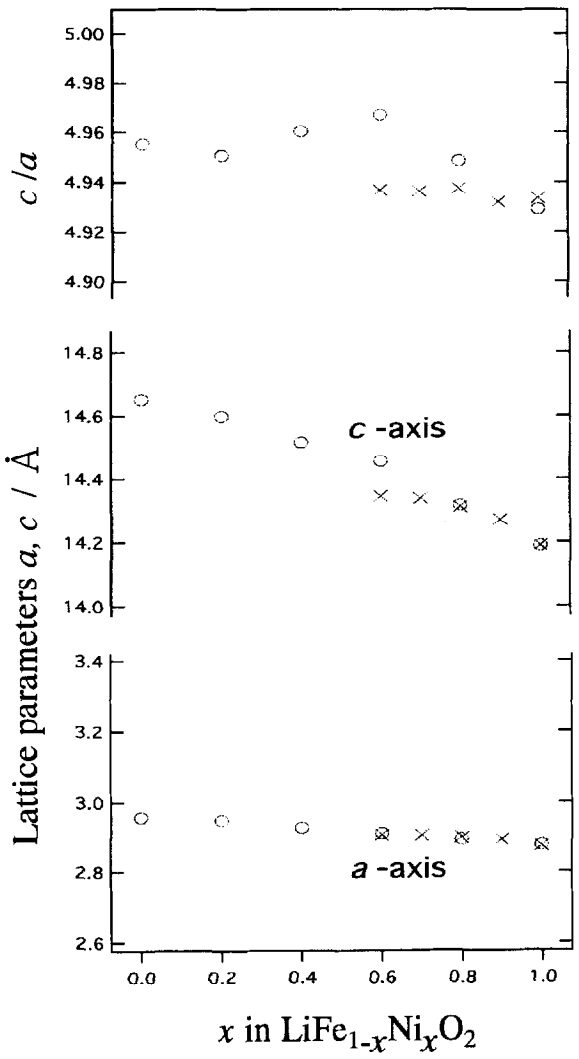

Fig. 6. Composition dependence of the lattice parameters and c/a ratio for $LiFe_{1-x}Ni_xO_2$ synthesized by (○) the ion-exchange reaction, and (×) solid state reaction.

tion, while the samples obtained by the direct synthesis have a small region of the layered structure. However, a deviation from the linear relationship was observed in the iron-rich region from $x=0.5$ to 0.0, which suggests an increase in cationic disordering.

Fig. 7 shows charge and discharge curves for the samples $LiFe_{1-x}Ni_xO_2$ synthesized by ion-exchange reaction. For the $LiFe_{1-x}Ni_xO_2$ cathodes, significant degradation with cycling was observed for the samples synthesized by the solid-state reaction [28], while no degradation was observed for the cathode synthesized by the ion-exchange reaction. The cationic disordering significantly affected their charge and discharge characteristics. Furthermore, cycling capacities of the 4 V region in the discharge curves decreased with increasing iron content.

3.3. $LiFeO_2$ with the corrugated layer structure

The ion-exchange reactions were conducted in sealed tubes under various reaction conditions using $LiOH \cdot H_2O$ and γ-FeOOH. Reactions between 120 and 250 °C gave the new phase together with α-$LiFeO_2$ and β-$LiFe_5O_8$. Higher reaction temperatures improved the crystallinity of the products. The composition was determined by inductive coupled plasma (ICP) spectroscopy for the sample synthesized by those conditions as follows: $LiOH \cdot H_2O$/γ-FeOOH ratio: 1.4/1.0; reaction temperatures: 200 °C; reaction time: 1 h. The molar ratio of the material was Li/Fe = 0.89, resulting in the formula, $Li_{0.94}Fe_{1.06}O_2$. The XRD pattern of the new phase is also quite similar to that of orthorhombic $LiMnO_2$ [22], and all reflections could be indexed using an orthorhombic cell; the cell parameters after refinement by Rietveld analysis were $a=4.0610(6$ Å), $b=2.9621(5$ Å), and $c=6.0319(12$ Å). The structure of $LiFeO_2$ was refined using XRD data from a structural model of orthorhombic $LiMnO_2$ [22]. The refinement results are summarized in Table 1. The Rietveld refinement results clearly indicate a mixed phase nature of the new orthorhombic phase and α-$LiFeO_2$. Furthermore, there is approximately 10% disorder in the cationic sites. In order to improve the sample quality, both the amount of α-$LiFeO_2$ and the cationic disorder in $LiFeO_2$ should be reduced. In γ-FeOOH, each Fe atom is surrounded by a distorted octahedral group of O atoms, and these groups are linked together to form corrugated layers [25].

The relationship between the reaction temperature and their structure are studied using an ion-exchange reaction between γ-FeOOH and LiOH in a sealed aluminum foil. The products contained α-$LiFeO_2$ as an impurity phase and the ratio, o-$LiFeO_2/LiFeO_2 + \alpha$-$LiFeO_2$, was refined by XRD data. The cation disorder in o-$LiFeO_2$ was also considered in the refinement in the lithium site using a structural model that disordered Fe ions in the Li site and the same amount of disordered Li ions in the Fe site. Fig. 8(a) shows the relationship between the reaction temperature and the ratio. The ratio increases with increasing reaction temperature and the highest ratio of ~0.87 was obtained for the synthesis temperature of 200 °C and reaction periods of 1–5 h. Fig. 8(b) shows the cationic disordering in the Li site versus reaction temperature. The disorder increases with increasing reaction temperature.

Fig. 9 shows the reaction temperature versus lattice parameters dependence for $LiFeO_2$. The lattice parameters vary with increasing reaction temperature; the a-parameter increases with increasing temperature from 80 to 220 °C, and the b- and c-parameters decrease with increasing temperature. The decrease in the c-parameter might be caused by the proton exchange to lithium; lower reaction temperatures might lead to insufficient ion exchange. Synthesis of pure $LiFeO_2$ with corrugated layer structure is rather difficult using the ion-exchange reaction from γ-FeOOH and $LiOH/LiOH \cdot H_2O$, because of the residual proton in the structure. Recently, a new synthesis route has been developed by Sakurai et al. [29]; $C_2H_5O \cdot Li$ (Li–EtOH) was used for the lithium source and an exchange reaction with γ-FeOOH in EtOH produced monophasic $LiFeO_2$. The lattice parameters of the phase obtained by the same method in the present study are

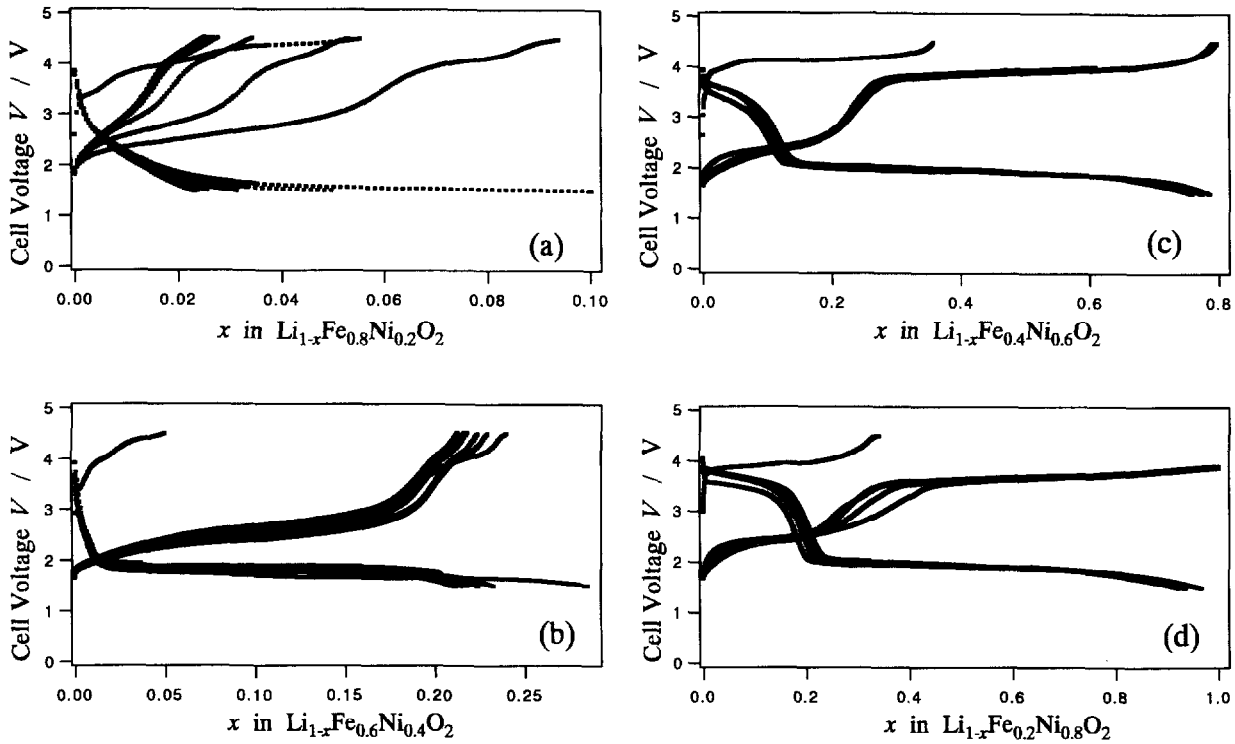

Fig. 7. Charge/discharge curves for $Li/LiFe_{1-x}Ni_xO_2$, using cathodes synthesized during the ion-exchange reaction.

Table 1
X-ray Rietveld refinement results for orthorhombic $LiFeO_2$ [a]

Atom	Site	g	x	y	z	B (Å^2)
Li(1)	2(a)	0.907(14)	0.25	0.25	0.109(8)	0.4(3)
Fe(1)	2(a)	0.093	0.25	0.25	$=z$(Li(1))	$=B$(Li(1))
Fe(2)	2(a)	0.907	0.25	0.25	0.6440(16)	$=B$(Li(1))
Li(2)	2(a)	0.093	0.25	0.25	$=z$(Fe(2))	$=B$(Li(1))
O(1)	2(b)	1.0	0.75	0.25	0.150(5)	$=B$(Li(1))
O(2)	2(b)	1.0	0.75	0.25	0.609(5)	$=B$(Li(1))

[a] Space group: *Pmmn*; $a=4.0610(5)$ Å; $b=2.9621(5)$ Å; $c=6.0319(11)$ Å; $R_{wp}=9.42$; $R_p=7.30$; $S=1.30$; $R_I=2.27$, and $R_F=1.30$. Mass fraction of compound, orthorhombic $LiFeO_2$:α-$LiFeO_2=0.77$:0.23.

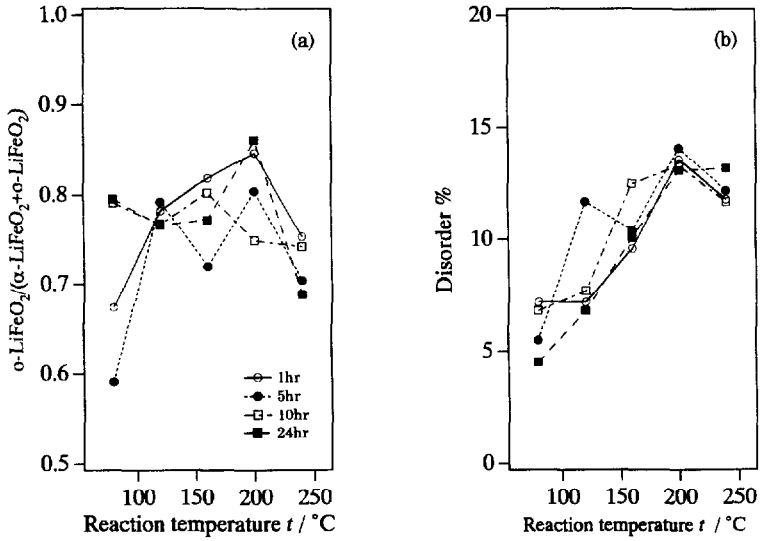

Fig. 8. (a) Relationship between the reaction temperatures and o-$LiFeO_2/o$-$LiFeO_2+\alpha$-$LiFeO_2$. (b) Relationship between the reaction temperatures and disorder.

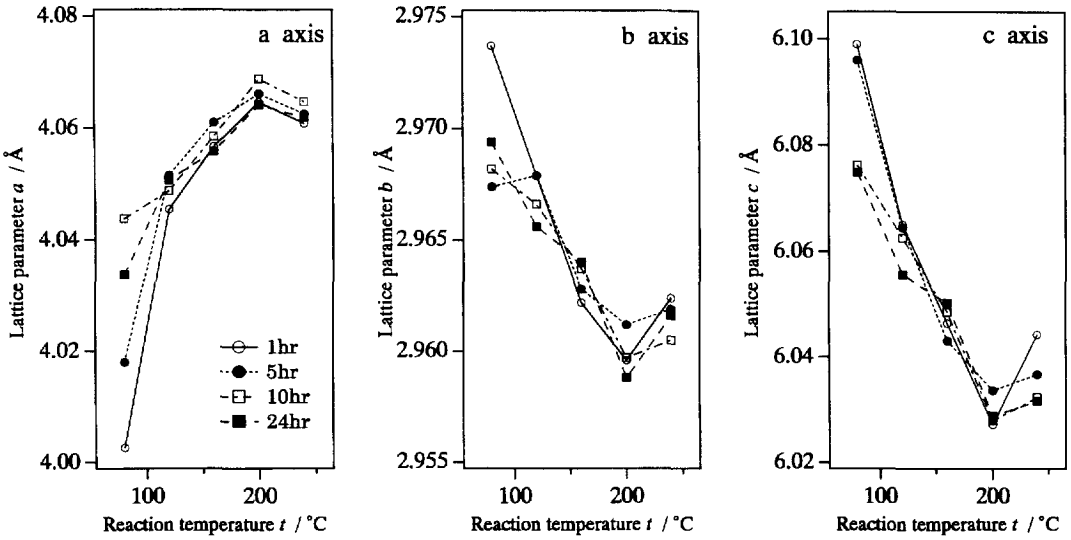

Fig. 9. Reaction temperature dependence of the lattice parameters of $LiFeO_2$ with the corrugated layer structure.

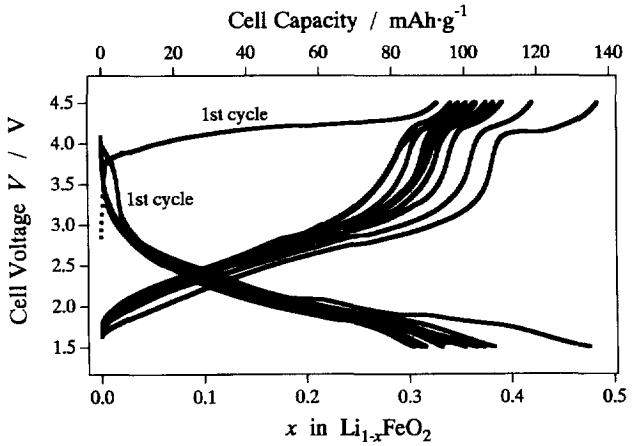

Fig. 10. Charge/discharge curves for the cells $Li/LiFeO_2$. Cut-off voltages were 4.2 V for charge and 1.5 V for discharge. Current density was 0.1 mA/cm^2 for charge and discharge.

$a=4.0302(10)$ Å, $b=2.9760(14)$ Å, $c=6.076(4)$ Å. This indicates that the exchange reaction is not completed at 80 °C for 12 h.

Charge/discharge experiments were carried out for the cells, $Li/LiFeO_2$; a sample used was that was synthesized under the ion-exchange conditions, $LiOH \cdot H_2O/\gamma$-FeOOH ratio: 1.4/1.0, reaction temperature: 200 °C, and reaction time: 1 h. The ratio of o-$LiFeO_2/\alpha$-$LiFeO_2$ determined by XRD Rietveld analysis was 77/23. Fig. 10 shows the charge and discharge curves for these cells. The electrode showed good reversibility in the limited composition range, $0.00 \leq x \leq 0.3$–0.4. In the first charge process, cell voltages increased rapidly to ~4 V and, then, increased slowly to 4.2 V. For discharge, however, cell voltages decreased rapidly to 3 V and then decreased slowly to the cut-off voltage, 1.5 V. The large difference in behavior between the first charge and discharge cycles might be caused by the complete structural change from the corrugated layer structure to an amorphous phase during the first charge process and probably by the difference in lithium site potential of these two phases.

In the isostructural orthorhombic $LiMnO_2$, conversion to a spinel structure occurs during the first few cycles in a lithium cell [30,31]. In the new orthorhombic $LiFeO_2$, the conversion proceeds from the corrugated layer structure to an amorphous phase; the '$LiFe_2O_4$' phase with the spinel structure might not be stable in the iron system due to exotic Fe^{4+}, which might cause lattice deformation leading to an amorphous phase. Charge and discharge after the second cycles proceeds in the amorphous phase. Only a slight decrease in cycling capacity was observed after the second cycle. This is the first example of a lithium iron oxide system which shows good electrode characteristics for lithium secondary cells. The amount of the corrugated layer phase in the cathodes were ~77%. The above results indicate that orthorhombic $LiFeO_2$ with a corrugated layer structure participates in the charge and discharge processes, and that the cycling capacity might increase in samples with higher purity and less cationic disorder.

Acknowledgements

This work was supported partly by a Grant-in-Aid for Scientific Research on Priority Areas (No. 260) from The Ministry of Education, Science and Culture, and a NEDO International Joint Research Grant.

References

[1] M.M. Thackeray, W.I.F. David, and J.B. Goodenough, *Mater. Res. Bull., 17* (1982) 785.
[2] M.S. Islam and C.R.A. Catlow, *J. Solid State Chem., 77* (1988) 180.
[3] M.M. Thackeray, W.I.F. David and J.B. Goodenough, *J. Solid State Chem., 55* (1984) 280.
[4] M. Pernet, P. Strobel, B. Bonnet, P. Bordet and Y. Chabre, *Solid State Ionics, 66* (1993) 259.
[5] L.A. de Picciotto and M.M. Thackeray, *Mater. Res. Bull., 21* (1986) 583.

[6] M.S. Whittingham, *Prog. Solid State Chem., 12* (1978) 41.
[7] Z. Takehara, H. Sakaebe and K. Kanaura, *J. Power Sources, 43–44* (1993) 627.
[8] S. Okada, H. Ohtsuka, H. Arai and M. Ichimura, *Proc. New Sealed Rechargeable Batteries and Supercapacitors,* Proc. Vol. 92-23, The Electrochemical Society, Los Angeles, CA, USA, 1993, p. 431
[9] A.K. Padhi, K.S. Nanjundaswamy and J.B. Goodenough, *Ext. Abstr., Meet. The Electrochemical Society,* Proc. Vol. 96-1, Pennington, NJ, USA, 1996, 73.
[10] L.P. Cardoso, D.E. Cox, T.A. Hewston and B.L. Chamberland, *J. Solid State Chem., 72* (1988) 234.
[11] A. Tauber, W.M. Moller and E. Banks, *J. Solid State Chem., 4* (1972) 138.
[12] K. Mizushima, P.C. Jones, P.J. Wiseman and J.B. Goodenough, *Mater. Res. Bull., 15* (1980) 783.
[13] M.H. Rossouw, D.C. Liles and M.M. Thackeray, *J. Solid State Chem., 104* (1993) 464.
[14] R. Kanno, H. Kubo, Y. Kawamoto, T. Kamiyama, F. Izumi, Y. Takeda and M. Takano, *J. Solid State Chem., 110* (1994) 216.
[15] A. Lecerf, *Ann. Chim., 7* (1962) 513.
[16] J.C. Anderon and M. Shieber, *J. Phys. Chem. Solids, 25* (1964) 961.
[17] R. Hoppe, *Bull. Soc. Chim. Fr., 1965* (1965) 1115.
[18] V. Nalbandyan and I. Sukaev, *Russian J. Inorg. Chem., 32* (1987) 453. English end.
[19] S. Kikkawa, H. Ohkura and M. Koizumi, *Mater. Chem. Phys., 18* (1987) 375.
[20] B. Fuchs and S. Kemmler-Sack, *Solid State Ionics, 68* (1994) 279.
[21] T. Shirane, R. Kanno, Y. Kawamoto, Y. Takeda, M. Takano, T. Kamiyama and F. Izumi, *Solid State Ionics, 79* (1995) 227.
[22] R. Hoppe, G. Brachtel and M. Jansen, *Z. Anorg. Allg. Chem., 417* (1975) 1.
[23] J.N. Reimers, E.W. Fuller, E. Rossen and J.R. Dahn, *J. Electrochem. Soc., 140* (1993) 3396.
[24] R.J. Gummow and M.M. Thackeray, *J. Electrochem. Soc., 141* (1994) 1178.
[25] A.F. Wells, *Structural Inorganic Chemistry*, Oxford University Press, London, 1984.
[26] R. Kanno, T. Shirane. Y. Kawamoto, Y. Takeda, M. Takano, M. Ohashi and Y. Yamaguchi, *J. Electrochem. Soc., 143* (1996) 2435.
[27] F. Izumi, in R.A. Young (ed.), *The Rietveld Method*, Oxford University Press, Oxford, 1993, Ch. 13.
[28] J.N. Reimers, E. Rossen, C.D. Jones and J.R. Dahn, *Solid State Ionics, 61* (1993) 335.
[29] Y. Sakurai, H. Arai and J. Yamaki, *Proc. Electrochemical Society of Japan, Spring Meet., Japan, 1996*, p. 108.
[30] R.J. Gummow, D.C. Liles and M.M. Thackeray, *Mater. Res. Bull., 28* (1993) 1249.
[31] I. Koetschau, M.N. Richard, J.R. Dahn, J.B. Soupart and J.C. Rousche, *J. Electrochem. Soc., 142* (1995) 2906.